ELSEVIER

Journal of Organometallic Chemistry 626 (2001) 125–138

Journal of Organometallic Chemistry

www.elsevier.nl/locate/jorganchem

Synthesis, characterisation, crystal structures and reactivity of a series of ruthenium–cobalt mixed-metal nitrido carbonyl clusters with iodide ligands

Emmie Ngai-Man Ho, Wing-Tak Wong *

Department of Chemistry, The University of Hong Kong, Pokfulam Road, Hong Kong, PR China

Received 31 October 2000; received in revised form 3 January 2001; accepted 3 January 2001

Abstract

Reaction of $[Ru_3(\mu\text{-}H)_2(CO)_9(\mu_3\text{-}NOMe)]$ (**1**) with two equivalents of $[Cp^*Co(CO)I_2]$ ($Cp^* = \eta^5\text{-}C_5Me_5$) in refluxing THF resulted in the isolation of four new heterometallic tetranuclear nitrido clusters, namely $[Ru_3CoH(\mu\text{-}H)(CO)_6(Cp^*)\{\mu\text{-}\eta^2\text{-}C(OMe)O\}(\mu_4\text{-}N)(\mu\text{-}I)_2]$ (**2**), $[Ru_3Co(\mu\text{-}H)_2(CO)_6(Cp^*)\{\mu\text{-}\eta^2\text{-}C(OMe)O\}(\mu_4\text{-}N)I(\mu\text{-}I)]$ (**3**), $[Ru_3Co(\mu\text{-}H)_2(CO)_6(Cp^*)\{\mu\text{-}\eta^2\text{-}C(OMe)O\}(\mu_4\text{-}N)I(\mu\text{-}I)]$ (**4**) and $[Ru_3Co(\mu\text{-}H)_2(CO)_8(\eta^5\text{-}C_5Me_5)(\mu_4\text{-}N)(\mu\text{-}I)]$ (**5**), together with a triruthenium nitrene cluster $[Ru_3(\mu\text{-}H)_3(CO)_8(\mu_3\text{-}NOMe)I]$ (**6**) in moderate yields. The first four clusters have either a chain (**2**) or a spiked triangle (**3**–**5**) metal skeleton with the central nitrido atom capping all four metal atoms; alternatively, these four clusters can also be viewed as having a highly distorted butterfly arrangement. Clusters **2**, **3** and **4** are isomers with different ligand dispositions. The hinge and an Ru–Ru wing-edge are missing in **2**, whereas a wing-edge is lost in each of **3** and **4** (Ru–Ru) and **5** (Ru–Co). Opening up the hinge metal–metal bond has a significant effect upon the nitrido chemical shift in the ^{15}N-NMR spectrum. Clusters **3** and **4** differ from each other in the coordination site of a terminal iodide ligand, and both clusters are inter-convertible under vigorous conditions. Cluster **6** is a trihydrido nitrene cluster with a terminal iodide ligand. ^{15}N-NMR studies were performed in order to investigate the environment of the nitrogen atoms in these nitrido and nitrene clusters.

Keywords: Ruthenium–cobalt; Cluster; Nitrido; Iodide; ^{15}N-NMR spectroscopy

1. Introduction

A number of organometallic species have been characterised, in which the tetrametallic frame has a 'butterfly' configuration [1]. This M_4 butterfly skeleton appears to be structurally versatile, and the geometry is determined by both the steric and electronic character of the ligands [2,3]. This finding has inspired intense theoretical and structural investigations [4]. Interesting reactivity patterns have been shown by butterfly clusters with nonclassical electron counts and geometries [5,6]. There are many examples of butterfly clusters containing small molecules of bare main group atoms coordinated within the cavity between the wing-tip atoms. The chemistry of the nitrido group in this 'semi-open' butterfly cluster framework is of great interest, since it provides a model system for study of the species formed during chemisorption of nitrogen and nitrogen compounds on bulk metal surfaces during heterogeneous catalysis [7]. There is growing evidence that mixed-metal systems may be more effective in some catalytic processes, as a suitable combination of different metals permits more efficient interactions with substrates than mononuclear metal complexes or their homometallic counterparts. It has been shown that the selectivity of cobalt-catalysed CO hydrogenation [8,9], and homologation of alcohols [10–12] and esters [13,14] is substantially improved by the addition of ruthenium derivatives. Furthermore, there is a beneficial influence of adding iodide ions on methanol carbonylation [15] and formate homologation [16] in the presence of Ru–Co catalysts. In addition, iodide has been demonstrated to be an effective promoter for the ligand-substitution reactions of $[Ru_3(CO)_{12}]$ [17,18].

* Corresponding author. Fax: +86-852-25472933 or +86-852-28571586.

E-mail address: wtwong@hkucc.hku.hk (W.-T. Wong).

0022-328X/01/$ - see front matter
PII: S0022-328X(01)00675-1

Therefore, investigation of Ru–Co mixed-metal clusters containing iodide ligands is of interest. Recently, we have developed reliable synthetic routes to mixed-metal butterfly clusters $[Ru_3Co(CO)_{12}(\mu_4\text{-N})]$, $[Ru_3Co(\mu\text{-H})(CO)_9(Cp^*)(\mu_4\text{-N})]$ and $[Ru_2Co_2(CO)_9(Cp^*)(\mu_4\text{-N})]$ [19]. In this paper we report the synthesis of a series of heteronuclear Ru_3Co nitrido clusters containing iodide ligands in the reaction between $[Ru_3(\mu\text{-H})_2(CO)_9(\mu_3\text{-NOMe})]$ (**1**) and $[Cp^*Co(CO)I_2]$.

2. Results and discussion

2.1. Synthesis, structure and spectroscopy

2.1.1. Reaction of **1** with $[Cp^*Co(CO)I_2]$

Heating compound **1** with $[Cp^*Co(CO)I_2]$ in refluxing THF for 1 h afforded a dark-brown mixture. Five new carbonyl clusters were isolated, in order of elution, $[Ru_3CoH(\mu\text{-H})(CO)_6(Cp^*)\{\mu\text{-}\eta^2\text{-C(OMe)O}\}(\mu_4\text{-N})(\mu\text{-I})_2]$ (**2**), $[Ru_3Co(\mu\text{-H})_2(CO)_6(Cp^*)\{\mu\text{-}\eta^2\text{-C(OMe)O}\}(\mu_4\text{-N})I(\mu\text{-I})]$ (**3**), $[Ru_3Co(\mu\text{-H})_2(CO)_8(Cp^*)(\mu_4\text{-N})(\mu\text{-I})]$ (**5**), $[Ru_3(\mu\text{-H})_3(CO)_8(\mu_3\text{-NOMe})I]$ (**6**) and $[Ru_3Co(\mu\text{-H})_2(CO)_6(Cp^*)\{\mu\text{-}\eta^2\text{-C(OMe)O}\}(\mu_4\text{-N})I(\mu\text{-I})]$ (**4**) in 13%, 12%, 20%, 10% and 17% yields respectively (Scheme 1). Clusters **2**–**6** were characterised by IR, ^{1}H- and ^{15}N-NMR spectroscopies and mass spectrometry (Table 1). Their structures were also established by single-crystal X-ray crystallography.

Clusters **2**–**5** all contain a butterfly-related Ru_3Co skeleton, with a nitrido ligand bonded to all four metal centres, and the three clusters **2**–**4** are geometrical isomers, having the same elemental composition. Cluster **2** differs from **3** and **4** in the number of metal–metal bonds (three M–M bonds in **2**, four in **3** and **4**), the coordination mode of the iodide ligands (two bridging iodides for **2**, one terminal and one bridging for both **3** and **4**) and the capping site of the –C(OMe)O group (hinge Ru–Ru bond for **2**, wing-edge Ru–Ru bond for **3** and **4**). The IR spectra of **2**–**4** reveal that only terminal carbonyl ligands are present. The positive FAB mass spectra displayed molecular ion peaks at m/z 994 and daughter ions due to successive loss of carbonyls. In the ^{1}H-NMR spectra, apart from the singlets due to the methoxy protons (δ 3.67–3.49) in the acetate moieties and the Cp* ligands (δ 1.83–1.81), there are two characteristic doublets in the hydride region each for **2**, **3** and **4**. At room temperature these sharp doublets indicate that the hydride ligands in clusters **2**–**4** are bonded only to the ruthenium atoms, because a hydrogen nucleus directly linked to cobalt gives a broad signal at 297 K due to the ^{59}Co quadrupole [20]. The nitrido N-atom in **2**, **3** and **4** gives a singlet in the corresponding ^{15}N-NMR spectrum at δ 371.0, 465.7 and 469.9.

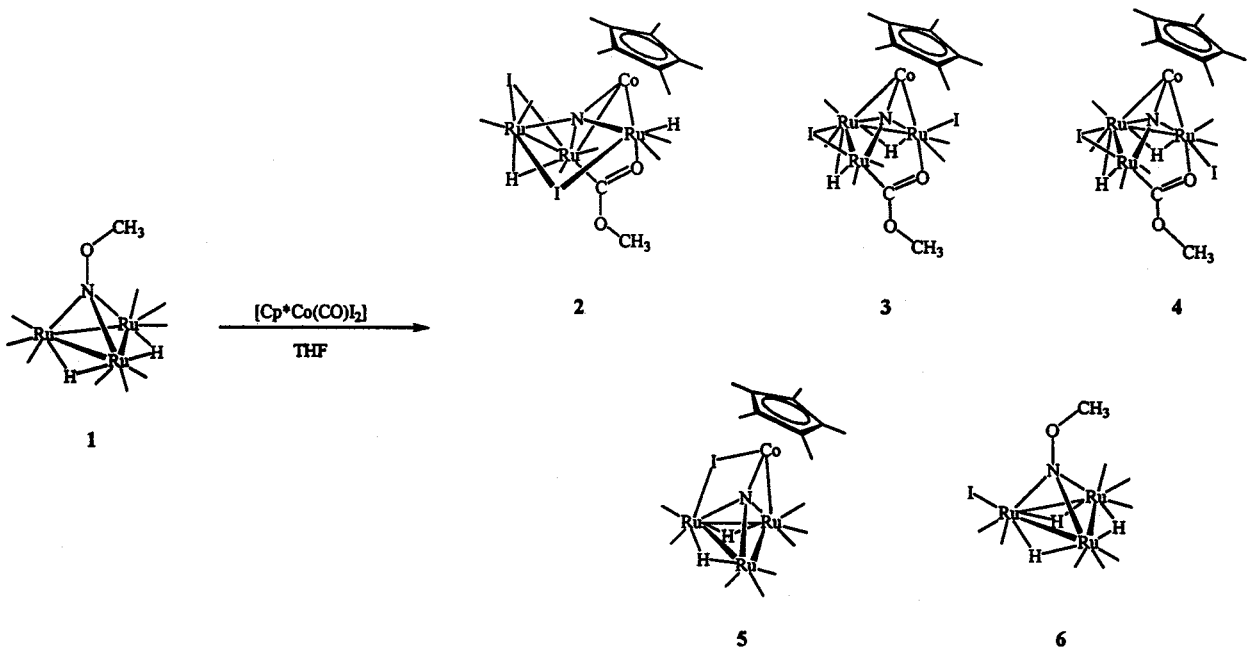

Scheme 1. Reaction of cluster **1** with 2 equiv. of $[Cp^*Co(CO)I_2]$ afforded in the isolation of five new compounds, three are isomers with formula of $[Ru_3CoH_2(CO)_6(Cp^*)\{\mu\text{-}\eta^2\text{-C(OMe)O}\}(\mu_4\text{-N})I_2]$ **2**, **3**, **4** and $[Ru_3Co(\mu\text{-H})_2(CO)_8(Cp^*)(\mu_4\text{-N})(\mu\text{-I})]$ **5** and $[Ru_3(\mu\text{-H})_3(CO)_8(\mu_3\text{-NOMe})I]$ **6** in moderate yields.

Table 1
Spectroscopic data for clusters **1**–**6**

Cluster	IR spectra[a] ν(CO)/cm^{-1}	^{1}H-NMR spectra[b] (δ, J/Hz)	^{15}N-NMR spectra[c] (δ, J/Hz)	Mass spectra[d] (m/z)
1	2116m, 2078s, 2057vs, 2048s, 2036sh, 2010vs, 2005s, 1988m	3.46 (s, 3H, methoxy) −17.22 (s, 2H, hydride)	301.0 (s)[e]	602 (602)
2	2078vw, 2070w, 2057m, 2039s, 2030vs, 1991m, 1983w, 1966w	3.49 (s, 3H, methoxy) 1.81 (s, 15H, C_5Me_5) −7.59 (d, J_{HH} = 2.1, 1H, hydride) −14.56 (d, J_{HH} = 2.1, 1H, hydride)	371.0 (s)	994 (994)
3	2066s, 2055vs, 2041s, 2005m, 1979m	3.52 (s, 3H, methoxy) 1.81 (s, 15H, C_5Me_5) −12.99 (d, J_{HH} = 2.1, 1H, hydride) −22.67 (d, J_{HH} = 2.1, 1H, hydride)	465.7 (s)	994 (994)
4	2062s, 2049vs, 2032s, 2003s, 1985s	3.67 (s, 3H, methoxy) 1.83 (s, 15H, C_5Me_5) −12.78 (d, J_{HH} = 2.7, 1H, hydride) −20.89 (d, J_{HH} = 2.7, 1H, hydride)	469.9 (s)	994 (994)
5	2087m, 2078m, 2057s, 2047vs, 2037s, 2016m, 2010m, 1997w, 1985w	**5′** 1.96 (s, 15H, C_5Me_5) −17.60 (br, 1H, hydride) −24.41 (br, 1H, hydride) **5″** 1.95 (s, 15H, C_5Me_5) −15.24 (br, 1H, hydride) −22.78 (br, 1H, hydride)	474.4 (s)	864 (864)
6	2122w, 2105s, 2059vs, 2053s, 2039w, 2003m	3.89 (s, 3H, methoxy) −17.64 (dd, J_{HH} = 2.1, 2.4,1H, hydride) −17.70 (dd, J_{HH} = 2.4, 2.7,1H, hydride) −19.17 (dd, J_{HH} = 2.1, 2.7,1H, hydride)	301.2 (s)	702 (702)

[a] In *n*-hexane.
[b] In CD_2Cl_2.
[c] In $CDCl_3$, with ^{1}H decoupled.
[d] Calculated values in parentheses.
[e] From Ref. [32].

The molecular structure of the tetranuclear mixed-metal nitrido cluster $[Ru_3CoH(\mu\text{-}H)(CO)_6(Cp^*)\{\mu\text{-}\eta^2\text{-}C(OMe)O\}(\mu_4\text{-}N)(\mu\text{-}I)_2]$ (**2**) is shown in Fig. 1, with selected interatomic distances and angles summarised in Table 2. In the solid state, the four metal atoms in cluster **2** define a chain metal core geometry. On the other hand, cluster **2** can be described as a butterfly with the hinge and one wing edge Ru–Ru bonds missing. To our knowledge, an Ru_4 butterfly metal core with a missing edge is rather rare, and the only example we are aware of is $[Ru_4(CO)_{12}(\mu_4\text{-}N)(\mu\text{-}OMe)]$, where no direct Ru–Ru interaction was found in the butterfly hinge [21]. The Cp*Co unit is at one of the wing-tips of the butterfly, opposite the iodide groups that bridge the Ru(1)–Ru(2) and Ru(2)–Ru(3) wing edges and the hydrido ligands, which also bridge the Ru(1)–Ru(2) bond,

and is terminally coordinated to the equatorial site of the Ru(3) atom. The metal–metal distances in $[Ru_3CoH(\mu\text{-}H)(CO)_6(Cp^*)\{\mu\text{-}\eta^2\text{-}C(OMe)O\}(\mu_4\text{-}N)(\mu\text{-}I)_2]$ (**2**) are in the range 2.645(1) to 2.950(2) Å. The longest and shortest ones are the Ru(1)–Co(1) and Ru(3)–Co(1) edges. The Ru(1)···Ru(3) and Ru(2)···Ru(3) separations (3.45 Å and 3.47 Å respectively) represent zero bond order, whereas these two edges are each bridged by the three-electron donor $\mu\text{-}\eta^2$-C(OMe)O and the μ-I group accordingly. The four M–N distances range from 1.770(7) to 2.128(7) Å, with the nitrido atom displaced towards Co(1). The Ru(1)–N(1)–Ru(3) and Ru(2)–N(1)–Co(1) angles are found to be 115.2(3)° and 155.1(4)° respectively, both of which deviate much from those found in cluster $[Ru_3Co(\mu\text{-}H)(CO)_9(Cp^*)(\mu_4\text{-}N)]$ [Ru(1)–N(1)–Ru(3) 83.1(1)° and Ru(2)–N(1)–Co(1) 175.0(2)°] [19]. The hinge bond is opened and all four metal atoms are folded upward relative to the nitrido atom. The Ru–I distances in **2** show an interesting variation, with the bond to Ru(2) [I(1)–Ru(2) 2.6787(9) and I(2)–Ru(2) 2.750(1) Å] being significantly shorter than to the hinge atoms Ru(1) or Ru(3) [I(1)–Ru(1) 2.8229(9) and I(2)–Ru(3) 2.804(1) Å]; the corresponding angles at these bridging iodide ligands are Ru(1)–I(1)–Ru(2) = 60.74(2)° and Ru(2)–I(2)–Ru(3) = 77.28(3)°. The former angle with I(1) is smaller, owing to a close interaction of Ru(1) and Ru(2). The ^{1}H-NMR spectrum of **2** shows two signals of equal intensity at δ −7.59 and −14.56, indicating different chemical environments for the hydrides. A mutual coupling between the hydride resonances with a coupling constant of 2.1 Hz was observed. Both of these hydrogen atoms were located from Fourier-difference maps. One of the hydrides occupies the wing Ru(1)–Ru(2) bond, and the other coordinates to Ru(3). Owing to the higher steric demand from the μ-I compared with the μ-H ligands, the bond angles Ru(2)–Ru(1)–C(1) and Ru(1)–Ru(2)–C(4) [152.1(3) and 141.7(3)°] are larger than those of Ru(2)–Ru(1)–C(2) and Ru(1)–Ru(2)–C(3) [112.8(3) and 120.2(3)°] The –C(OMe)O ligand caps the Ru(1)–Ru(3) hinge through a σ bonding interaction with C(7) to Ru(1) [2.01(1) Å] and a σ bonding interaction with O(7) to Ru(3) [2.136(7) Å]. The O(7)–C(7) bond [1.22(1) Å] is slightly longer and the O(7)–C(7)–O(8) angle [118.3(9)°] slightly smaller than those (average 1.1875 Å and 123.5°) in the carbamate moieties reported previously [22,23], whilst the data of the carbomethoxy group is well consistent with those in $[Ru_6(CO)_{13}(\mu\text{-}CO)(\mu_3\text{-}NH)(\mu_5\text{-}N)(\mu_3\text{-}OMe)\{\mu\text{-}\eta^2\text{-}C(O)OMe\}_2]$ [24]. The formation of this $\mu\text{-}\eta^2$-carbomethoxy moiety seems to involve the coupling of the metal-bounded methoxy group originating from the

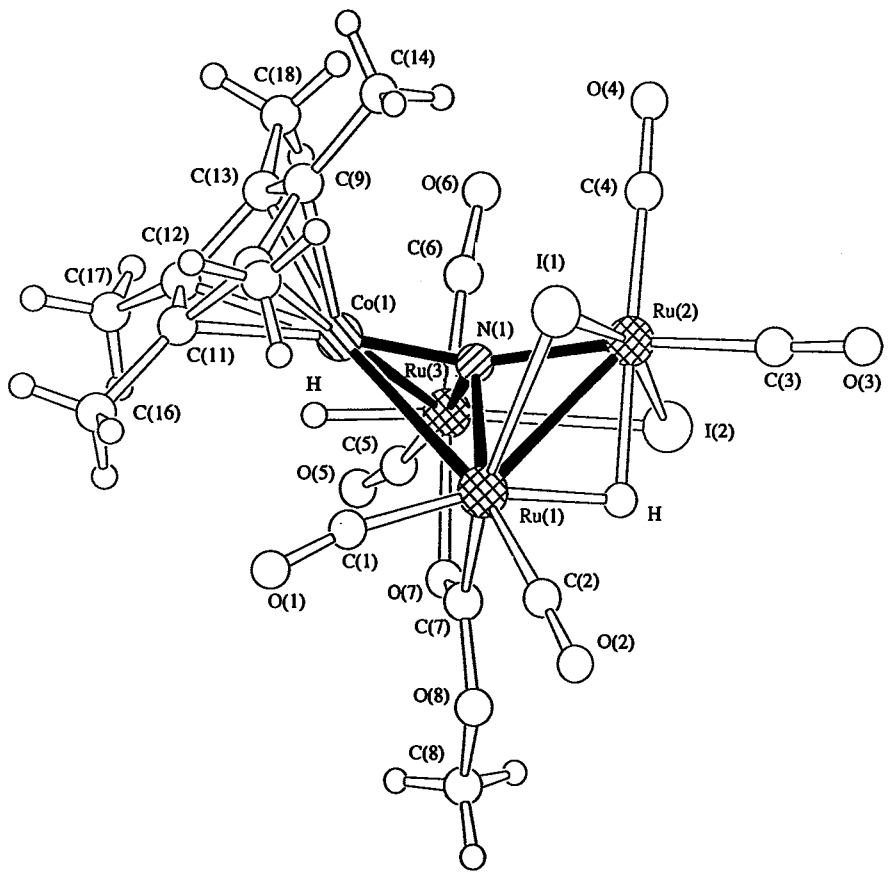

Fig. 1. The molecular structure of $[Ru_3CoH(\mu\text{-}H)(CO)_6(Cp^*)\{\mu\text{-}\eta^2\text{-}C(OMe)O\}(\mu_4\text{-}N)(\mu\text{-}I)_2]$ (**2**) with the atom numbering scheme.

Table 2
Selected bond lengths (Å) and angles (°) for clusters **2** and **4**; the values in square brackets refer to the second independent molecule of **4**

	2	**4**	
I(1)–Ru(1)	2.8229(9)	2.754(2)	[2.748(2)]
I(1)–Ru(2)	2.6787(9)	2.797(3)	[2.804(2)]
I(2)–Ru(2)	2.750(1)	–	–
I(2)–Ru(3)	2.804(1)	2.697(2)	[2.721(2)]
Ru(1)–Ru(2)	2.7844(9)	2.748(3)	[2.764(2)]
Ru(1)–Ru(3)	–	2.828(3)	[2.812(2)]
Ru(1)–Co(1)	2.950(2)	2.827(3)	[2.817(3)]
Ru(1)–N(1)	2.128(7)	2.11(1)	[2.07(1)]
Ru(1)–C(7)	2.01(1)	–	–
Ru(2)–N(1)	2.044(7)	2.02(2)	[2.05(1)]
Ru(2)–C(7)	–	1.99(2)	[1.97(2)]
Ru(3)–Co(1)	2.645(1)	2.634(3)	[2.624(2)]
Ru(3)–O(7)	2.136(7)	2.12(1)	[2.162(10)]
Ru(3)–N(1)	2.066(7)	2.04(2)	[2.04(1)]
Co(1)–N(1)	1.770(7)	1.74(1)	[1.73(1)]
O(7)–C(7)	1.22(1)	1.26(2)	[1.25(2)]
O(8)–C(7)	1.35(1)	1.34(2)	[1.35(2)]
O(8)–C(8)	1.44(1)	1.49(3)	[1.42(2)]
Co(1)–Cp*(c)[a]	1.701	1.676	1.688
Ru(1)–I(1)–Ru(2)	60.74(2)	59.34(6)	[59.71(4)]
Ru(2)–I(2)–Ru(3)	77.28(3)	–	–
Ru(2)–Ru(1)–Ru(3)	–	77.73(7)	[77.97(5)]
Ru(2)–Ru(1)–Co(1)	80.97(3)	81.82(8)	[82.49(6)]
Ru(2)–Ru(1)–N(1)	46.9(2)	46.8(4)	[47.5(4)]
Ru(3)–Ru(1)–Co(1)	–	55.51(7)	[55.58(6)]
Ru(3)–Ru(1)–N(1)	–	46.0(4)	[46.3(4)]
Co(1)–Ru(1)–N(1)	36.5(2)	38.0(4)	[37.8(3)]
Ru(1)–Ru(2)–N(1)	49.4(2)	49.7(4)	[48.1(4)]
I(2)–Ru(3)–Co(1)	124.36(4)	151.80(10)	[150.24(7)]
Ru(1)–Ru(3)–Co(1)	–	62.23(8)	[62.30(7)]
Ru(1)–Ru(3)–N(1)	–	48.0(4)	[47.2(4)]
Co(1)–Ru(3)–N(1)	41.9(2)	41.4(4)	[41.3(3)]
Ru(1)–Co(1)–Ru(3)	78.32(4)	62.26(8)	[62.12(6)]
Ru(1)–Co(1)–N(1)	45.6(2)	48.1(5)	[46.9(5)]
Ru(3)–Co(1)–N(1)	51.3(2)	50.7(5)	[50.9(4)]
Ru(3)–O(7)–C(7)	122.4(6)	123(1)	[120(1)]
C(7)–O(8)–C(8)	117.2(9)	117(1)	[119(1)]
Ru(1)–N(1)–Ru(2)	83.7(3)	83.5(6)	[84.5(5)]
Ru(1)–N(1)–Ru(3)	115.2(3)	85.9(5)	[86.5(5)]
Ru(1)–N(1)–Co(1)	97.9(3)	94.0(6)	[95.3(6)]
Ru(2)–N(1)–Ru(3)	115.1(3)	119.3(7)	[118.5(6)]
Ru(2)–N(1)–Co(1)	155.1(4)	152.4(10)	[153.6(8)]
Ru(3)–N(1)–Co(1)	86.8(3)	87.9(7)	[87.8(6)]
Ru(1)–C(7)–O(7)	125.5(7)	–	–
Ru(1)–C(7)–O(8)	116.2(8)	–	–
Ru(2)–C(7)–O(7)	–	122(1)	[125(1)]
Ru(2)–C(7)–O(8)	–	119(1)	[119(1)]
O(7)–C(7)–O(8)	118.3(9)	117(2)	[114(1)]

[a] Cp*(c) denotes the centroid of the C_5Me_5 ring.

methoxynitrido ligand in **1** and the coordinated carbonyl ligand. Apart from acting as model compounds for studying the coordination of the carbomethoxy moiety present in the homogeneous homologation of methyl acetate by $[Ru_3Co(CO)_{13}]^-$ and $[RuCo_3(CO)_{12}]^-$ [13], this complex may also provide some insight into the methanol carbonylation to give acetic acid [25]. In addition, these discrete molecular nitrido clusters are thought to be more stable, especially towards the temperatures and pressures required for catalytic reactions. The nitrido atom can be viewed as a central spring that enhances the integrity of the cluster, while also providing the flexibility needed for its activity in catalysis, and is now regarded as a new kind of catalytic promoter. The metallocyclic pentagon with Ru(1), N(1), Ru(3), O(7) and C(7) is essentially planar, with maximum deviations of 0.062 Å from the least-squares plane. The μ-η^2-C(OMe)O, μ-I(1), μ-I(2) and terminal hydride ligands in **2** are placed in a trans configuration consecutively. The μ-I and the μ-η^2-C(OMe)O ligands are both regarded as three-electron donors [26]; hence a cluster valence electron (CVE) count of 66 results, which is consistent with a tetranuclear cluster with only three metal–metal bonds.

The molecular structures of $[Ru_3Co(\mu\text{-}H)_2(CO)_6(Cp^*)\{\mu\text{-}\eta^2\text{-}C(OMe)O\}(\mu_4\text{-}N)I(\mu\text{-}I)]$ (**3**, **4**) are depicted in Figs. 2 and 3 with key bond distances and angles listed in Tables 3 and 2 respectively. The metal cores of clusters **3** and **4** are both composed of a rare spiked triangular arrangement of Ru_3Co atoms. Some related examples are the tetraosmium clusters reported by Pomeroy and co-workers [26]. Besides, the μ-η^2-C(OMe)O fragments bridge the other open Ru–Ru wing edges and the second iodide ligands coordinate to the hinge Ru(3) terminally. An obvious structural difference in **3** and **4** compared with **2** is that bonding interactions are present between the hinge atoms, which are also bridged by hydride ligands. The isomers **3** and **4** only differ from each other with respect to the coordination sites of the terminal iodide on Ru(3). The iodide occupies an equatorial site in **3** and an axial site in **4**. The structural difference between clusters **3** and **4** is that the terminal iodide is in cis configuration to Co(1) in **3** and trans configuration in **4**.

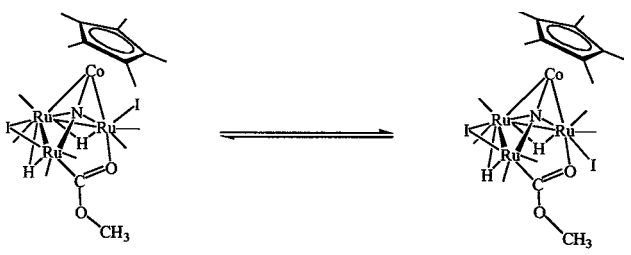

3 **4**

interconversion between clusters **3** and **4**

In the structure determination of **3**, extensive disorder was encountered due to the presence of both enantiomeric forms of **3** crystallised in the lattice, thus generating a pseudo-mirror plane, even though the molecule of **3** does not contain a mirror symmetry. Such a mirror plane is found to coincide with the crystallographic mirror plane in the space group $P2_1/m$ (no. 11). The Co(1), N(1), O(4), C(9) and C(12) atoms lie on the mirror plane. Apart from the Ru(1), Co(1), I(1), N(1), O(1), O(2), O(4), C(1), C(2), C(7), C(8), C(10) and C(11) atoms, all others were refined with an occupancy factor of 0.5. However, there are two independent molecules of **4** in an asymmetric unit, and only one of them is shown in Fig. 3. Both clusters **3** and **4** have the same metal framework, with a distorted butterfly arrangement of Ru_3Co missing an Ru–Ru wing edge. The Cp* ligands bind to the Co(1) atom with distances of 1.699 Å for **3** and 1.676 and 1.688 Å for **4**, which do not differ much from that of **2** [Co–Cp* 1.701 Å]. The longest M–M bond in both **3** and **4** is the Ru(1)–Ru(3) hinge [2.767(2) Å for **3**, 2.828(3) and 2.812(2) Å for **4**], which is also capped by a bridging hydride. The three other M–M bonds formed by the wing-tip and hinge metal atoms are in the ranges 2.649(2)–2.764(2) Å for **3** and 2.624(2)–2.827(3) Å for **4**, whereas the shortest contacts are Ru(1)–Ru(2) [2.649(2) Å] in **3** and Ru(3)–Co(1) [2.634(3) and 2.624(2) Å] in **4**. The non-bonding distances of the missing wing edge are 3.64 Å for **3** and 3.50 and 3.51 Å for **4**, and these edges are capped by a three-electron μ-η^2-C(OMe)O moiety. The planes defined by Ru(2), N(1), Ru(3) and the corresponding ketyl group in the μ-η^2-C(OMe)O ligands are essentially planar, with mean deviations from the least-squares plane of 0.216 Å (**3**), 0.142 and 0.135 Å (**4**). The nitrido nitrogen atom bonds to the four metal atoms and is tilted towards Co(1), with distances of 1.75(1) Å for **3** and 1.74(1) and 1.73(1) Å for molecules of **4**. The unique Ru–Ru wing edges in both **3** and **4** are bridged equatorially by iodide and axially by hydride ligands. The terminal iodide ligand coordinates to Ru(1*) with a 2.706(1) Å bond distance in **3**, and to Ru(3) with 2.697(3) and 2.721(2) Å distances in **4**; all are shorter than the Ru–I distances involving the bridging I(1) atoms. The bridging iodide and the –C(OMe)O ligands are arranged in trans configuration in **3** and **4**. Each molecule of **3** and **4** has two hydride ligands, which are evident from its ^{1}H-NMR spectrum. The observed chemical shift values are typical of hydrido ligands occupying bridging positions

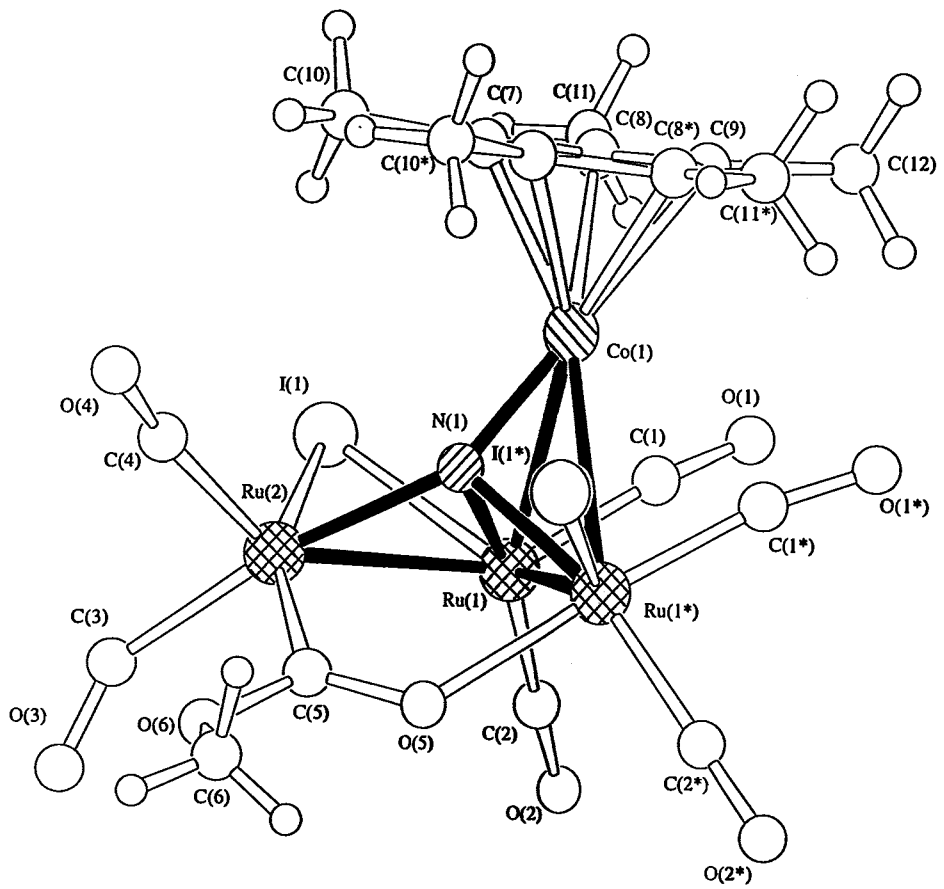

Fig. 2. The molecular structure of $[Ru_3Co(\mu\text{-}H)_2(CO)_6(Cp^*)\{\mu\text{-}\eta^2\text{-}C(OMe)O\}(\mu_4\text{-}N)I(\mu\text{-}I)]$ (**3**) with the atom numbering scheme.

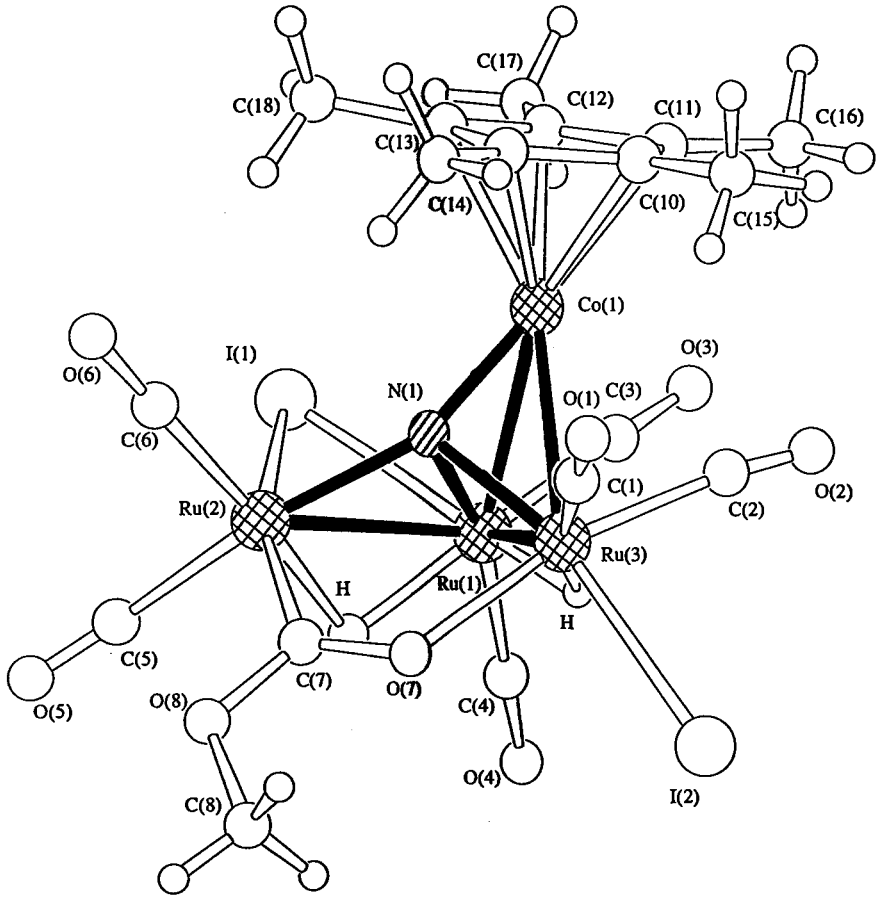

Fig. 3. The molecular structure of $[Ru_3Co(\mu\text{-}H)_2(CO)_6(Cp^*)\{\mu\text{-}\eta^2\text{-}C(OMe)O\}(\mu_4\text{-}N)I(\mu\text{-}I)]$ (**4**) with the atom numbering scheme.

in the cluster [**3**: δ −12.99 (d, J_{HH} = 2.1 Hz), δ −22.67 (d, J_{HH} = 2.1 Hz); **4**: δ −12.78 (d, J_{HH} = 2.7 Hz), δ −20.89 (d, J_{HH} = 2.7 Hz)]; the signal at higher field correlates well with other hinged-bridging hydrides in clusters with a butterfly geometry [27]. Owing to the absence of broadening of the hydride signals at room temperature associated with a ^{59}Co quadrupole (I = 7/2), these two hydrides are believed to be placed along the two Ru–Ru bonds. Hydrides in cluster **4** were located from the Fourier-difference maps, whereas the locations of hydrides in **3** could not be determined from X-ray analysis due to the extensive disorder associated with the crystal. The molecular structures of **3** and **4** differ from that of **2** by a metal–metal bond in the hinge, and in the possession of a terminal iodide rather than a bridging one. Electron counting indicates that both **3** and **4** have 64 valence electrons, which is consistent with a spiked triangular skeleton with four M–M bonds [28]. The change in bonding mode of bridging (**2**) to terminal (**3** and **4**) is accompanied by a decrease from three to one of the number of electrons the ligand donates to complex bonding. The iodide ligands readily form bridges, which are easily broken in reactions with other ligands. This is the important role of iodides in the catalytic processes.

Cluster **4** was found to be interconvertible with **3** under vigorous reaction conditions. The isolated product distribution was the same, within experimental error, whether the reaction started from cluster **3** or cluster **4**, and also included cluster **5**, which was also obtained in low yield. Owing to the large size of the iodide ligand, its scrambling process and that of the two carbonyl ligands on the same Ru atom requires a high activation energy, whereas the formation energies for **3** and **4** should be similar as they were obtained in nearly the same amounts.

The fourth product isolated in this reaction was $[Ru_3Co(\mu\text{-}H)_2(CO)_8(Cp^*)(\mu_4\text{-}N)(\mu\text{-}I)]$ (**5**). Complex **5** also contains an Ru_3CoI core, as evidenced by both the molecular ion peaks and isotopic distribution from its mass spectrum (Table 1). Its IR spectrum shows CO stretching frequencies corresponding to terminal carbonyls only. The ^{1}H-NMR data at room temperature are consistent with the solid-state structures containing one Cp* and two bridging hydride ligands. ^{15}N-NMR studies of the ^{15}N-enriched samples of **5** gave a singlet at δ 474.4. In order to establish the molecular structure of **5**, the compound has been characterised by X-ray crystallographic analysis (Fig. 4). Selected bond

parameters are given in Table 4. The molecular geometry of cluster **5** is similar to that of **3** and **4**, in that the four metal atoms are also arranged as a spiked triangle or a highly distorted butterfly with a wing edge missing. In **5** the missing edge is one of the Ru–Co bonds, instead of an Ru–Ru bond as in **3** and **4**. This non-bonding Ru–Co edge was a separation of 3.21 Å and is subsequently bridged by an iodide ligand. The Cp* ligand is distant from Co(1) at 1.680 Å. The hinge metal–metal contact [2.834(1) Å] is found to be the longest, whereas the other wing edges are of lengths 2.773(1) Å [Ru(1)–Ru(2)], 2.750(1) Å [Ru(2)–Ru(3)] and 2.792(2) Å [Ru(3)–Co(1)]. The nitrido N bonds all the four metal atoms, and is displaced towards Co(1) with a distance of 1.792(7) Å. The iodide ligand is only partially transferred to the Ru cluster, unlike the case of clusters **2**–**4**. I(1) bridges the Ru(1) [I(1)–Ru(1) 2.736(1) Å] and Co(1) [I(1)–Co(1) 2.718(1) Å] atoms and the corresponding angle is 72.16(4)° [Ru(1)–I(1)–Co(1)]. The presence of two isomers of **5** was shown by the ^{1}H-NMR study, with two sets of broad hydride signals being observed at room temperature. Cluster **5** exists as two isomers (**5′** and **5″**) with differences in the positions of the bridging hydride ligands in the solution state. The ^{1}H-NMR spectrum of **5** at −60°C contains a set of sharp hydride signals at δ −25.36 and −17.21 for **5′** and another set at δ −22.90 and −15.24 for **5″**, with relative intensities in the ratio of 6:1. The presence of the two isomers can be accounted for, as the wing-edge-bridged hydride occupies each of the two non-equivalent Ru–Ru wing edges.

Table 3
Selected bond lengths (Å) and angles (°) for cluster **3**

I(1)–Ru(1)	2.706(1)
I(1)–Ru(2)	2.891(2)
Ru(1)–Ru(1*)	2.767(2)
Ru(1)–Ru(2)	2.649(2)
Ru(1)–Co(1)	2.764(2)
Ru(1*)–O(5)	2.18(1)
Ru(1)–N(1)	2.067(10)
Ru(2)–N(1)	2.12(1)
Ru(2)–C(5)	1.96(2)
Co(1)–N(1)	1.75(1)
O(5)–C(5)	1.28(2)
O(6)–C(5)	1.34(3)
O(6)–C(6)	1.90(4)
Co(1)–Cp*(c)[a]	1.699
Ru(1)–I(1)–Ru(2)	56.38(4)
Ru(1*)–Ru(1)–Ru(2)	84.45(5)
Ru(1*)–Ru(1)–Co(1)	59.97(3)
Ru(1*)–Ru(1)–N(1)	48.0(2)
Ru(2)–Ru(1)–Co(1)	85.46(7)
Ru(2)–Ru(1)–N(1)	51.6(3)
Co(1)–Ru(1)–N(1)	39.2(4)
I(1*)–Ru(1*)–Co(1)	92.28(4)
Ru(1)–Ru(2)–N(1)	49.9(3)
Ru(1)–Co(1)–Ru(1*)	60.06(6)
Ru(1)–Co(1)–N(1)	48.3(3)
Ru(1)–O(5)–C(5)	125(1)
C(5)–O(6)–C(6)	122(1)
Ru(1)–N(1)–Ru(1*)	84.0(5)
Ru(1)–N(1)–Ru(2)	78.6(3)
Ru(1)–N(1)–Co(1)	92.5(5)
Ru(2)–N(1)–Co(1)	143.7(4)
Ru(2)–C(5)–O(5)	122(1)
Ru(2)–C(5)–O(6)	120(1)
O(5)–C(5)–O(6)	116(1)

[a] Cp*(c) denotes the centroid of the C_5Me_5 ring.

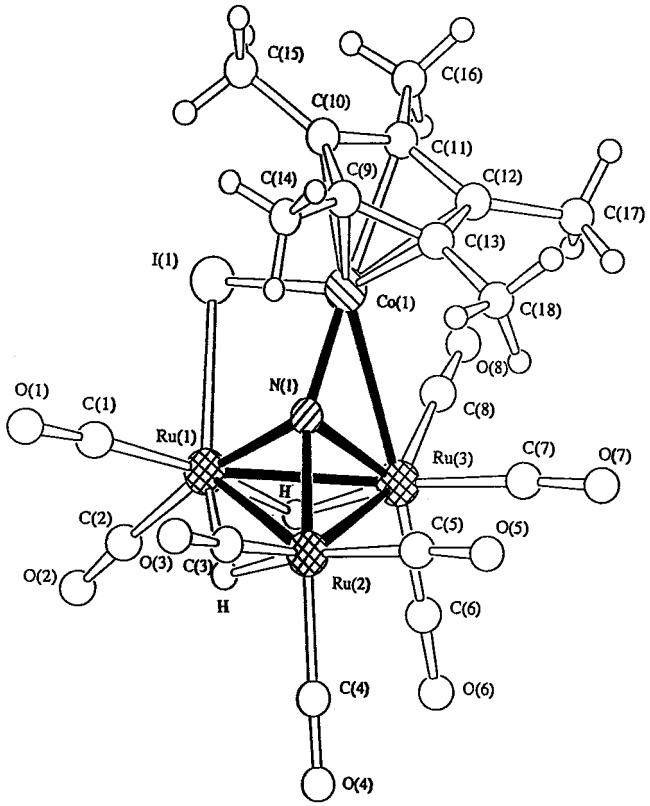

Fig. 4. The molecular structure of $[Ru_3Co(\mu\text{-}H)_2(CO)_8(Cp^*)(\mu_4\text{-}N)(\mu\text{-}I)]$ (**5**) with the atom numbering scheme.

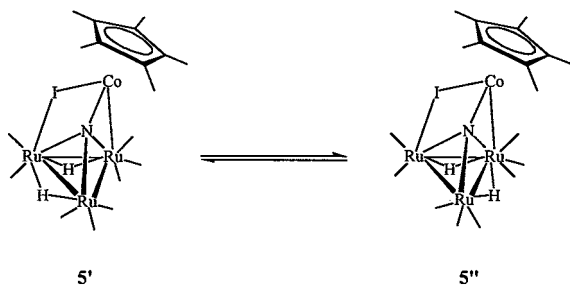

isomerisation between 5' and 5"

At −20°C the bridging hydride resonances start to broaden. As the solution is gradually warmed to +50°C, the hydride signals coalesce to two broad singlets at δ −23.92 and −17.79. At or above this temperature, fast exchange of the wing-edge-bridged hydride ligand takes place. In each set of ^{1}H-NMR signals there

should be one hydride bridging the hinge and the other bridging an Ru–Ru wing edge [29], accompanied by a Cp* ligand signal. In the solid-state structure the hydrides were located directly from the Fourier-difference map and placed at the Ru(1)–Ru(2) and Ru(1)–Ru(3) bonds [2.773(1) Å and 2.834(1) Å], which are significantly longer than Ru(2)–Ru(3) [2.750(1) Å]. Furthermore, space-filling models [29] show that steric demand from the hydride ligands results in the opening up of the Ru–Ru–CO angles along the Ru(1)–Ru(2) edge. The bond angles Ru(2)–Ru(1)–C(2) [128.8(3)°] and Ru(1)–Ru(2)–C(4) [114.4(3)°] are larger than the angles Ru(3)–Ru(2)–C(4) [107.7(4)°] and Ru(2)–Ru(3)–C(6) [95.5(4)°]. It is believed that the isomeric structure **5′** is thermodynamically more stable than **5″**, and more abundant in the solution state. The Ru(2)–N(1)–Co(1) bond angle [158.6(4)°] deviates significantly from linearity, and the Ru(1)–N(1)–Ru(3) angle becomes 86.3(2)°. With a three-electron donor μ-I ligand, cluster **5** has a CVE count similar to the 64 of **3** and **4**.

The final product isolated in this reaction is cluster **6**, which is a trihydrido methoxynitrido triruthenium carbonyl cluster with a terminal iodide ligand. The molecular structure of **6** is given in Fig. 5, and selected bond lengths and angles are in Table 5. Cluster **6** consists of an isosceles triangular Ru_3 core, capped by μ_3-NOMe and three bridging hydride ligands. The iodide is terminally bonded to one Ru atom in an orientation trans to a μ-H ligand, with a distance of 2.701(2) Å. When compared with the parent cluster **1**, one terminal iodide and one bridging hydride replace a terminal carbonyl ligand in **1**. The three Ru–Ru bond distances are 2.821(2), 2.792(2) and 2.838(2) Å, with the shortest distance corresponding to the Ru(1)–Ru(3) bond trans to the I^- ligand. Each Ru(1) and Ru(2) atom is linked to two 'equatorial' carbonyl ligands, whereas Ru(3) has only one, which is trans to the μ-hydride ligands. Each of the Ru atoms bonds to one 'axial' carbonyl ligand, which is trans to the μ_3-methoxynitrido nitrogen, N(1). The methoxynitrido ligand is bound to the triruthenium framework via the bonds Ru(1)–N(1) 2.02(1) Å, Ru(2)–N(1) 2.04(1) Å and Ru(3)–N(1) 2.06(1) Å; the Ru(1)–N(1)–Ru(2), Ru(1)–N(1)–Ru(3) and Ru(2)–N(1)–Ru(3) angles are 88.2(4)°, 86.4(4)° and 87.6(4)° respectively. Each of these values is comparable to those in cluster **1** [21]. From the ^{1}H-NMR spectrum of **6**, a methoxy signal is observed at δ 3.89, in addition to three double doublets at δ −17.64, −17.70 and −19.17 with integral ratios of 3:1:1:1, proving that the three bridging hydrides undergo mutual coupling. The NOMe moiety is inclined toward Ru(2), as is evident from the values of Ru(1)–N(1)–O(9) 128.8(8)°, Ru(2)–N(1)–O(9) 119.3(9)° and Ru(3)–N(1)–O(9) 132.6(9)°. The N–O bond distance is 1.40(1) Å, and the O(9)–C(9) bond distance is 1.47(2) Å. The N(1)–O(9)–C(9) angle is 110(1)°. Three hydride ligands were directly located in the crystallographic study, each bridging an Ru–Ru edge. The bridging hydrides lie in the expected position between the axial and equatorial carbonyl ligands below the plane of the cluster, on the opposite side of the molecule to the organic ligand. This arrangement is close to that found in $[Ru_3(\mu\text{-}H)_3(CO)_9(\mu_3\text{-}CMe)]$ [30] and $[Ru_3(\mu\text{-}H)_3(CO)_9(\mu_3\text{-}CCl)]$ [31], in which the hydrogen atoms are nearly trans to the equatorial CO. Owing to the presence of an asymmetrically coordinated terminal iodide ligand, these three hydrides are not equivalent, having different chemical shifts in their ^{1}H-NMR spectra.

Table 4
Selected bond lengths (Å) and angles (°) for cluster **5**

I(1)–Ru(1)	2.736(1)
I(1)–Co(1)	2.718(1)
Ru(1)–Ru(2)	2.773(1)
Ru(1)–Ru(3)	2.834(1)
Ru(1)–N(1)	2.041(7)
Ru(2)–Ru(3)	2.750(1)
Ru(2)–N(1)	1.984(7)
Ru(3)–Co(1)	2.792(2)
Ru(3)–N(1)	2.101(7)
Co(1)–N(1)	1.792(7)
Co(1)–Cp*(c)[a]	1.680
Ru(1)–I(1)–Co(1)	72.16(4)
Ru(2)–Ru(1)–Ru(3)	58.74(3)
Ru(2)–Ru(1)–N(1)	45.6(2)
Ru(3)–Ru(1)–N(1)	47.7(2)
Ru(1)–Ru(2)–Ru(3)	61.75(3)
Ru(1)–Ru(2)–N(1)	47.3(2)
Ru(3)–Ru(2)–N(1)	49.5(2)
Ru(1)–Ru(3)–Ru(2)	59.51(3)
Ru(1)–Ru(3)–Co(1)	69.64(3)
Ru(1)–Ru(3)–N(1)	45.9(2)
Ru(2)–Ru(3)–Co(1)	84.06(4)
Ru(2)–Ru(3)–N(1)	45.9(2)
Co(1)–Ru(3)–N(1)	39.9(2)
Ru(3)–Co(1)–N(1)	48.8(2)
Ru(1)–N(1)–Ru(2)	87.1(3)
Ru(1)–N(1)–Ru(3)	86.3(2)
Ru(1)–N(1)–Co(1)	113.7(3)
Ru(2)–N(1)–Ru(3)	84.6(3)
Ru(2)–N(1)–Co(1)	158.6(4)
Ru(3)–N(1)–Co(1)	91.3(3)

[a] Cp*(c) denotes the centroid of the C_5Me_5 ring.

2.2. ^{15}N-NMR spectroscopy

^{15}N-NMR spectroscopy is a useful technique in studying the geometry of clusters. The ^{15}N-NMR data for a series of homo- and hetero-metallic nitrido/nitrene clusters have been investigated [19]. This included the chemical shifts for some Ru_3Co nitrido butterfly clusters, which are believed to be informative for making comparisons with data for the highly distorted butterfly Ru_3Co nitrido clusters obtained in this study. All of the

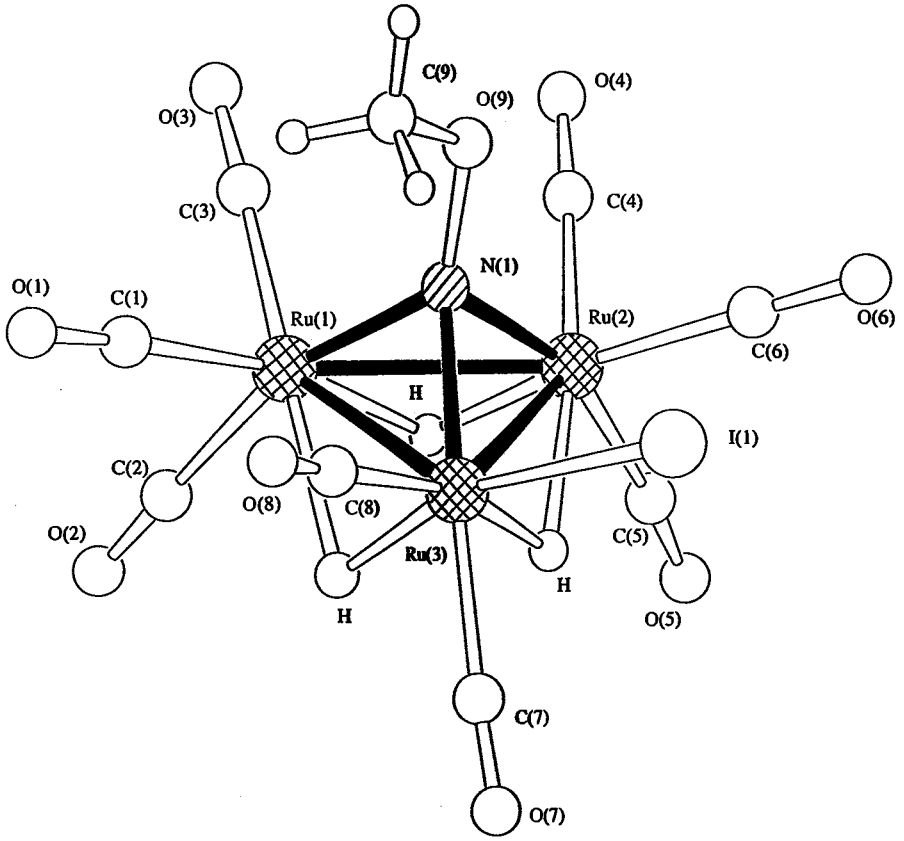

Fig. 5. The molecular structure of $[Ru_3(\mu\text{-}H)_3(CO)_8(\mu_3\text{-}NOMe)I]$ (**6**) with the atom numbering scheme.

clusters **2**–**6** in this study were examined by ^{15}N-NMR spectroscopy. Table 1 summarises the nitrogen chemical shifts obtained.

Cluster **1**, which is formed by the hydrogenation of $[Ru_3(CO)_9(\mu_3\text{-}CO)(\mu_3\text{-}NOMe)]$, exhibits a singlet at δ 301.0 (reference: liquid NH_3) in its $^{15}N\text{-}\{^1H\}$-NMR spectrum [32]. In the nucleophilic substitution reaction of $[Ru_3(CO)_9(\mu_3\text{-}CO)(\mu_3\text{-}NOMe)]$ with [PPN][$Co(CO)_4$], the butterfly nitrido cluster $[Ru_3Co(CO)_{12}(\mu_4\text{-}N)]$ (Co: hinge) was isolated in high yield and gave a resonance at 494.5 ppm. Upon replacement of a wing-tip $Ru(CO)_3$ group by an isolobal Cp*Co moiety, a 30.2 ppm downfield shift was observed in the resulting cluster $[Ru_2Co_2(CO)_9(Cp^*)(\mu_4\text{-}N)]$ (2Co: hinge and wing-tip). In the reaction between **1** and $[Cp^*Co(CO)_2]$ [19], a butterfly nitrido cluster $[Ru_3Co(\mu\text{-}H)(CO)_9(Cp^*)(\mu_4\text{-}N)]$ (Co: wing-tip) was also isolated in high yield. The nitrido N-atom resonated at δ 481.1. Another cluster, $[Ru_6Co(\mu_3\text{-}H)(CO)_8(\mu\text{-}CO)_3(\mu_4\text{-}\eta^2\text{-}CO)(Cp^*)_3(\mu_4\text{-}N)]$ (Co: wing-tip), formed in this reaction is an expanded form of the previous compound formed by further coordination of a triruthenium chain on the Ru_3 wing face, which displays a downfield shift of 68 ppm. In all these above-mentioned clusters, the nitrido nitrogen was placed in a butterfly metal skeleton. Clusters **2** and

Table 5
Selected bond lengths (Å) and angles (°) for cluster **6**

I(1)–Ru(3)	2.701(2)
Ru(1)–Ru(2)	2.821(2)
Ru(1)–Ru(3)	2.792(2)
Ru(1)–N(1)	2.02(1)
Ru(2)–Ru(3)	2.838(2)
Ru(2)–N(1)	2.04(1)
Ru(3)–N(1)	2.06(1)
N(1)–O(9)	1.40(1)
O(9)–C(9)	1.47(2)
Ru(2)–Ru(1)–Ru(3)	60.75(4)
Ru(2)–Ru(1)–N(1)	46.2(3)
Ru(3)–Ru(1)–N(1)	47.5(3)
Ru(1)–Ru(2)–Ru(3)	59.12(4)
Ru(1)–Ru(2)–N(1)	45.6(3)
Ru(3)–Ru(2)–N(1)	46.5(3)
Ru(1)–Ru(3)–Ru(2)	60.13(4)
Ru(1)–Ru(3)–N(1)	46.1(3)
Ru(2)–Ru(3)–N(1)	45.8(3)
N(1)–O(9)–C(9)	110(1)
Ru(1)–N(1)–Ru(2)	88.2(4)
Ru(1)–N(1)–Ru(3)	86.4(4)
Ru(1)–N(1)–O(9)	128.8(8)
Ru(2)–N(1)–Ru(3)	87.6(4)
Ru(2)–N(1)–O(9)	119.3(9)
Ru(3)–N(1)–O(9)	132.6(9)

Table 6
M_wNM_w and M_hNM_h bond angles[a] for butterfly and related clusters

Cluster	δ (^{15}N) (ppm)	r(N)[b] (pm)	M_wNM_w (°)	M_hNM_h (°)
$[Ru_3Co(\mu\text{-}H)(CO)_9(\eta^5\text{-}C_5Me_5)(\mu_4\text{-}N)]$ [19]	481.1	58.9	175.0	83.1
2	371.0	60.6	155.1	115.2
3	465.7	63.3	143.7	84.0
4	469.9	59.7	152.4, 153.6	85.9, 86.5
5	474.4	58.6	158.6	86.3

[a] M_w: wing-tip metal; M_h: hinge metal.
[b] The interstitial nitrogen radius r(N) [$= r(MN)_{ave} - r(MM)_{ave}/2$] [33] for nitrido clusters.

5 in this study are all highly distorted Cp^*CoRu_3 (Co: wing-tip) butterfly clusters containing iodide ligands, which can be viewed as having chain or spiked triangular structures. One wing-edge is absent in the last three complexes (Ru–Ru edge for **3** and **4**, Ru–Co edge for **5**), whereas the chemical shifts (δ 465.7–474.4) of the ^{15}N-atoms do not differ much from the most closely similar perfect butterfly cluster $[Ru_3Co(\mu\text{-}H)(CO)_9(Cp^*)(\mu_4\text{-}N)]$ [19] (δ 481.1). Some compression is relieved by the deviation from linearity of the M_wNM_w bonds, where M_w is a wingtip metal (Table 6), and there is a pleasing correlation of this angle with the interstitial shift. The Ru_wNCo_w angle decreases from 175.0° in $[Ru_3Co(\mu\text{-}H)(CO)_9(Cp^*)(\mu_4\text{-}N)]$ [19] to 158.6° in **5**, 152.4° and 153.6° in **4**, and 143.7° in **3**, the nitrogen shielding increasing over a range of 15.4 ppm, as compression is relieved. The interstitial radius r(N) [33] of nitrogen (Table 6) in clusters **3**–**5** also decreases gradually, which further supports the relief of compression by flapping the wings. In these three clusters, the Ru_hNRu_h angles do not deviate much from those of 'real' butterflies (Table 6). However, upon further opening up of the hinge metal–metal bond, the nitrogen resonance of **2** undergoes a significant shift to a high field value of δ 371.0. Cluster **2** is an anomaly, with an usual interstitial radius of the nitrogen, $r(N) = 60.6$ pm, but it gives an exceptional upfield ^{15}N resonance. The Ru_hNRu_h angle of **2** is equal to 115.2°, which is much larger than that of $[Ru_3Co(\mu\text{-}H)(CO)_9(Cp^*)(\mu_4\text{-}N)]$ (83.1°) [19]. This highly distorted butterfly cluster shows a further shielding–decompression correlation, involving the M_hNM_h angle. Opening-up the Ru_hNRu_h angle has a significant shielding effect on the interstitial. The M_wNM_w change of 31.3° in **3** (relative to $[Ru_3Co(\mu\text{-}H)(CO)_9(Cp^*)(\mu_4\text{-}N)]$ [19]) has only increased the shielding by 15.4 ppm, whereas the M_hNM_h change of 32.1° (together with M_wNM_w change of 19.9°) gives a very noticeable high field shift of 110.1 ppm for cluster **2**. The ^{15}N-NMR measurements made in this study on these four tetranuclear nitrido clusters are the first to be reported for butterfly complexes with distorted metal skeletons. $[Ru_3(\mu\text{-}H)_3(CO)_8(\mu_3\text{-}NOMe)I]$ (**6**) is very similar to the starting cluster **1**, with only a single carbonyl ligand replaced by an one-electron terminal iodide and a bridging hydride ligand. There is no serious influence on the chemical and magnetic environment of the ^{15}N atoms.

3. Experimental

3.1. General procedures

All reactions and manipulations were carried out under argon using standard Schlenk techniques, except for the chromatographic separations. Solvents were purified by standard procedures and distilled prior to use. All chemicals, unless otherwise stated, were purchased commercially and used as received. $[Ru_3(\mu\text{-}H)_2(CO)_9(\mu_3\text{-}NOMe)]$ [32], $[Ru_3(CO)_9(\mu_3\text{-}CO)(\mu_3\text{-}NOMe)]$ [34] and $[PPN][^{15}NO_2]$ [35] were prepared by the literature methods. Reactions were monitored by analytical thin-layer chromatography (TLC; Merck Kieselgel 60 F_{254}) and the products were separated by TLC on plates coated with silica (Merck Kieselgel 60 GF_{254}). IR spectra were recorded on a Bio-Rad FTS-7 IR spectrometer, using 0.5 mm calcium fluoride solution cells. ^{1}H-NMR spectra were recorded on a Bruker DPX300-NMR spectrometer using CD_2Cl_2 and referenced to $SiMe_4$ ($\delta = 0$), ^{15}N-NMR spectra were collected on a Bruker DPX500-NMR spectrometer using $CDCl_3$ solvent with liquid NH_3 as reference. Positive and negative ions fast atom bombardment (FAB) mass spectra were recorded on a Finnigan MAT 95 mass spectrometer, using *m*-nitrobenzyl alcohol or α-thioglycerol as matrix solvents. Microanalyses were performed by Butterworth Laboratories, UK.

3.2. Reaction of *1* with *[Cp*Co(CO)I$_2$]*

Complex **1** (200 mg, 0.33 mmol) and $[Cp^*Co(CO)I_2]$ (316.3 mg, 0.66 mmol) were dissolved in THF (50 ml). The dark-purple solution was heated at 65°C for 1 h, which resulted in the formation of a deep-brown solution. The solvent was removed under reduced pressure and the residue separated by preparative TLC using the eluent *n*-hexane/CH_2Cl_2 (3:1, v/v). Five products were isolated in the following order of elution, $[Ru_3CoH(\mu\text{-}$

H)(CO)$_6$(Cp*){μ-η^2-C(OMe)O}(μ$_4$-N)(μ-I)$_2$] (**2**) (R_f 0.65, 42.9 mg, 0.043 mmol, 13%), [Ru$_3$Co(μ-H)$_2$(CO)$_6$(Cp*){μ-η^2-C(OMe)O}(μ$_4$-N)I(μ-I)] (**3**) (R_f 0.50, 39.6 mg, 0.040 mmol, 12%), [Ru$_3$Co(μ-H)$_2$(CO)$_8$(Cp*)(μ$_4$-N)(μ-I)] (**5**) (R_f 0.45, 57.4 mg, 0.066 mmol, 20%), [Ru$_3$(μ-H)$_3$(CO)$_8$(μ$_3$-NOMe)I] (**6**) (R_f 0.28, 23.3 mg, 0.033 mmol, 10%) and [Ru$_3$Co(μ-H)$_2$(CO)$_6$(Cp*){μ-η^2-C(OMe)O}(μ$_4$-N)I(μ-I)] (**4**) (R_f 0.25, 56.1 mg, 0.056 mmol, 17%).

Anal. Found: C, 21.8; H, 1.9; N, 1.3. Calc. for $C_{18}H_{20}NO_8I_2CoRu_3$ (**2**): C, 21.73; H, 2.01; N, 1.41%. Found: C, 21.6; H, 2.2; N, 1.4. Calc. for $C_{18}H_{20}NO_8I_2CoRu_3$ (**3**): C, 21.73; H, 2.01; N, 1.41%. Found: C, 25.3; H, 1.8; N, 1.4. Calc. for $C_{18}H_{17}NO_8ICoRu_3$ (**5**): C, 25.00; H, 1.97; N, 1.62%. Found: C, 15.5; H, 1.0; N, 1.8. Calc. for $C_9H_6NO_9IRu_3$ (**6**): C, 15.38; H, 0.85; N, 1.99%. Found: C, 21.5; H, 2.1; N, 1.5. Calc. for $C_{18}H_{20}NO_8I_2CoRu_3$ (**4**): C, 21.73; H, 2.01; N, 1.41%.

3.3. Thermolysis of complex *3* in n-heptane

A solution of compound **3** (20 mg, 0.020 mmol) in *n*-heptane (20 ml) was refluxed under argon for 3 h. The colour of the reaction mixture darkened gradually. The solvent was removed in vacuo and the residue chromatographed on silica using *n*-hexane/CH_2Cl_2 (3:1, v/v) as eluent. Three consecutive bands were eluted. The first brown band was unchanged **3** (R_f 0.50, 5.0 mg, 0.005 mmol, 25%). The following products eluted were **5** (R_f 0.45, 2.09 mg, 0.0024 mmol, 12%) and **4** (R_f 0.25, 6.0 mg, 0.006 mmol, 30%).

3.4. Thermolysis of complex *4* in n-heptane

Compound **4** (20 mg, 0.020 mmol) was dissolved in *n*-heptane (20 ml). The brown solution was then heated to reflux and the reaction monitored by spot TLC. The mixture was dried under reduced pressure and the residue chromatographed on silica TLC plates using *n*-hexane/chloromethane (3:1, v/v) as eluent. Compounds **3** (R_f 0.50, 5.6 mg, 0.0056 mmol), **5** (R_f 0.45, 1.7 mg, 0.002 mmol) and **4** (R_f 0.25, 6.0 mg, 0.006 mmol) were eluted in sequence with 28%, 10% and 30% yields respectively.

3.5. Crystallography

Crystals suitable for X-ray analyses were glued on glass fibres with epoxy resin or sealed in 0.3 mm glass capillaries. Intensity data were collected at ambient temperature either on a Rigaku-AFC7R diffractometer (complex **5**) or a MAR research image plate scanner (complexes **2**–**4** and **6**) equipped with graphite-monochromated Mo-K$_\alpha$ radiation ($\lambda = 0.710\,73$ Å) using ω–2θ and ω scan types respectively. Details of the

Table 7
Crystal data and data collection parameters for compounds **2**–**6**

	2	**3**·$CHCl_3$	**4**	**5**	**6**·0.5CH_2Cl_2
Empirical formula	$C_{18}H_{20}NO_8I_2CoRu_3$	$C_{19}H_{21}NO_8I_2Cl_3CoRu_3$	$C_{18}H_{20}NO_8I_2CoRu_3$	$C_{18}H_{17}NO_8ICoRu_3$	$C_{9.5}H_7NO_9IClRu_3$
Formula weight	994.31	1113.69	994.31	864.38	744.73
Crystal colour, habit	Dark Green, block	Brown, block	Dark brown, block	Dark brown, block	Yellow, block
Crystal dimensions (mm^3)	0.21 × 0.31 × 0.41	0.12 × 0.32 × 0.34	0.34 × 0.16 × 0.14	0.19 × 0.11 × 0.18	0.33 × 0.35 × 0.43
Crystal system	Monoclinic	Monoclinic	Orthorhombic	Triclinic	Triclinic
Space group	$P2_1/c$ (# 14)	$P2_1/m$ (# 11)	$Pbca$ (# 61)	$P\bar{1}$ (# 2)	$P\bar{1}$ (# 2)
a (Å)	10.022(1)	8.785(1)	17.919(2)	10.125(3)	8.637(1)
b (Å)	16.416(2)	15.424(2)	18.709(2)	15.231(3)	8.701(1)
c (Å)	16.628(2)	12.718(1)	32.425(2)	9.235(3)	14.753(2)
α (°)				96.07(2)	83.04(1)
β (°)	103.20(2)	112.17(2)		116.39(2)	76.12(1)
γ (°)				93.26(2)	72.22(1)
U (Å^3)	2663.4(6)	1595.9(4)	10 870(1)	1260.0(7)	1023.5(2)
Z	4	2	16	2	2
Density (calc) (g cm^{-3})	2.480	2.313	2.430	2.278	2.416
μ(Mo–K$_\alpha$) (cm^{-1})	46.41	41.28	45.48	36.77	38.61
Diffractometer	MAR Research Image Plate	MAR Research Image Plate	MAR Research Image Plate	Rigaku AFC7R	MAR Research Image Plate
Reflections collected	22 595	17 302	33 834	3496	9880
Unique reflections	5092	2897	9875	3272	3261
Observed reflections [$I > 1.5\sigma(I)$]	4006	1814	6117	2382	2588
R	0.048	0.060	0.066	0.037	0.067
R'	0.052	0.062	0.068	0.039	0.091
Goodness of fit S	1.96	1.15	1.28	1.24	2.56

intensity data collection and crystal data are given in Table 7. The diffracted intensities were corrected for Lorentz and polarization effects. The Ψ scan method was employed for semi-empirical absorption corrections for **5** [36]. However, an approximation to absorption correction by inter-image scaling was applied for **4** and **6**. Scattering factors were taken from Ref. [37a] and anomalous dispersion effects [37b] were included in F_c. The structures were solved by direct methods (SIR92 [38] for **3**, SHELX86 [39] for **5** and **6**, and DIRDIF [40] for **2** and **4**) and expanded by Fourier-difference techniques. Atomic coordinates and thermal parameters were refined by full-matrix least-squares analysis on F, with the ruthenium atoms and non-hydrogen atoms being refined anisotropically, except for cluster **3**. Only ruthenium, cobalt, iodine and chlorine atoms are refined anisotropically. Metal hydrides were located by Fourier-difference synthesis, whereas those of the organic moieties were generated in their ideal positions (C–H 0.95 Å). Calculations were performed on a Silicon Graphics computer, using the program package TEXSAN [41].

4. Supplementary material

Crystallographic data (excluding structure factors) for the structures reported in this paper have been deposited with the Cambridge Crystallographic Data Centre (CCDC) as supplementary publication nos CCDC 149458–CCDC 149462. Copies of the data can be obtained free of charge on application to CCDC, 12 Union Road, Cambridge CB2 1EZ, UK (fax: +44-1223-336033; e-mail: deposit@ccdc.cam.ac.uk).

Acknowledgements

We gratefully acknowledge financial support from the Hong Kong Research Grants Council and the University of Hong Kong. E.N.-M. Ho acknowledges the receipt of a postgraduate studentship, Swire Scholarship 1998–2000, Hung Hing Ying Scholarship 1998–2000 and Epson Foundation Scholarship 2000–2001 administered by the University of Hong Kong and Michael Gale Scholarship 1998–99 awarded by the University of Hong Kong and Hong Kong Telecom Foundation.

References

[1] E. Sappa, A. Tiripicchio, A.J. Carty, G.E. Toogood, Prog. Inorg. Chem. 35 (1987) 437.
[2] A.J. Carty, S.A. MacLaughlin, J. van Wagner, N.J. Taylor, Organometallics 1 (1982) 1013.
[3] G. Hogarth, J.A. Phillips, F. van Gastel, N.J. Taylor, T.B. Marder, A.J. Carty, J. Chem. Soc. Chem. Commun. (1988) 1570.
[4] D. Osella, M. Ravera, C. Nervi, C.E. Housecroft, P.R. Raithby, P. Zanello, F. Laschi, Organometallics 10 (1991) 3253.
[5] R.D. Adams, L.W. Yang, J. Am. Chem. Soc. 104 (1982) 4115.
[6] R.D. Adams, L.W. Yang, J. Am. Chem. Soc. 105 (1983) 235.
[7] A. Ozaki, K. Aika, Catal. Sci. Technol. 1 (1981) 87.
[8] J. Kiviaho, M. Reinikainen, M.K. Niemelä, K. Kataja, S. Jääskeläinen, J. Mol. Catal. A: Chem. 106 (1996) 187.
[9] M. Reinikainen, J. Kiviaho, M. Kröger, M.K. Niemelä, S. Jääskeläinen, J. Mol. Catal. A: Chem. 118 (1997) 137.
[10] T. Matsuzaki, Y. Sugi, H. Arakawa, K. Takeuchi, K.-I. Bando, N. Isogai, Chem. Ind. (1985) 555.
[11] G. Jenner, P. Andrianary, J. Mol. Catal. 58 (1990) 307.
[12] K.-I. Tominaga, Y. Sasaki, T. Watanabe, M. Saito, Advances in Chemical Conversions for Mitigating Carbon Dioxide, Studies in Surface Science and Catalysis, vol. 114, Elsevier Science, 1998, pp. 495–498.
[13] M. Hidai, Y. Koyasu, M. Yokota, M. Orisaku, Y. Uchida, Bull. Chem. Soc. Jpn. 55 (1982) 3951.
[14] G. Jenner, J. Mol. Catal. A: Chem. 96 (1995) 215.
[15] T. Mizoroki, T. Matsumoto, A. Ozaki, Bull. Chem. Soc. Jpn. 52 (1979) 479.
[16] E. Kolehmainen, K. Rissanen, K. Laihia, Z.A. Kerzina, M.I. Rybinskaya, M. Nieger, J. Organomet. Chem. 524 (1996) 219.
[17] S.-H. Han, G.L. Geoffroy, A.L. Rheingold, Inorg. Chem. 26 (1987) 3426.
[18] G. Lavigne, H.D. Kaesz, J. Am. Chem. Soc. 106 (1984) 4647.
[19] E.N.-M. Ho, Z. Lin, W.-T. Wong, Eur. J. Inorg. Chem. (2001) in press.
[20] T. Saito, S. Sawada, Bull. Chem. Soc. Jpn. 58 (1985) 459.
[21] K.K.-H. Lee, W.-T. Wong, J. Chem. Soc. Dalton Trans. (1996) 1707.
[22] E.N.-M. Ho, W.-T. Wong, J. Chem. Soc. Dalton Trans. (1998) 513.
[23] E.N.-M. Ho, W.-T. Wong, J. Chem. Soc. Dalton Trans. (1998) 4215.
[24] K.K.-H. Lee, W.-T. Wong, Inorg. Chem. 35 (1996) 5393.
[25] (a) D. Forster, Adv. Organomet. Chem. 17 (1979) 255. (b) D. Forster, J. Am. Chem. Soc. 98 (1976) 846.
[26] (a) F.W.B. Einstein, L.R. Martin, R.K. Pomeroy, P. Rushman, J. Chem. Soc. Chem. Commun. (1985) 345. (b) L.R. Martin, F.W.B. Einstein, R.K. Pomeroy, Organometallics 7 (1988) 294. (c) F.W.B. Einstein, V.J. Johnston, A.K. Ma, R.K. Pomeroy, Organometallics 9 (1990) 52. (d) F.W.B. Einstein, V.J. Johnston, R.K. Pomeroy, Organometallics 9 (1990) 2754.
[27] M.A. Collins, B.F.G. Johnson, J. Lewis, J.M. Mace, J. Morris, M. McPartlin, W.J.H. Nelson, J. Puga, P.R. Raithby, J. Chem. Soc. Chem. Commun. (1983) 689.
[28] D.M.P. Mingos, Acc. Chem. Res. 17 (1984) 311.
[29] K. Henrick, M. McPartlin, J. Morris, Angew. Chem. 98 (1986) 843; Angew. Chem. Int. Ed. Engl. 25 (1986) 853.
[30] M.S. George, P.Y. James, J. Chem. Soc. Dalton Trans. (1975) 873.
[31] N.J. Zhu, C. Lecomte, P. Coppens, J.B. Keister, Acta Crystallogr. Sect. B 38 (1982) 1286.
[32] J.A. Smieja, R.E. Stevens, D.E. Fjare, W.L. Gladfelter, Inorg. Chem. 24 (1985) 3206.
[33] (a) J. Mason, J. Am. Chem. Soc. 113 (1991) 24. (b) J. Mason, J. Am. Chem. Soc. 113 (1991) 6056.
[34] R.E. Stevens, W.L. Gladfelter, J. Am. Chem. Soc. 104 (1982) 6454.
[35] R.E. Stevens, W.L. Gladfelter, Inorg. Chem. 22 (1983) 2034.
[36] A.C.T. North, D.C. Phillips, F.S. Mathews, Acta Crystallogr. Sect. A 24 (1968) 351.
[37] D.T. Cromer, J.T. Waber, International Tables for X-ray Crystallography, vol. 4, Kynoch Press, Birmingham, 1974, p. 2 (b) Table 2.2B; (b) Table 2.3.1.

[38] A. Altomare, M.C. Burla, M. Camalli, M. Cascarano, C. Giacovazzo, A. Guagliardi, G. Polidori, J. Appl. Crystallogr. 25 (1992) 310.
[39] G.M. Sheldrick, in: G.M. Sheldrick, C. Kruger, R. Goddard (Eds.), Crystallographic Computing 3, Oxford University Press, 1985, p. 175.
[40] P.T. Beurskens, G. Admiraal, G. Beurskens, W.P. Bosman, S. Garcia-Granda, R.O. Gould, J.M.M. Smits, C. Smykalla, The DIRDIF program system, Technical Report of the Crystallography Laboratory University of Nijmegan, The Netherlands, 1992.
[41] TEXSAN, Crystal Structure Analysis Package, Molecular Structure Corporation, Houston, TX, 1985 and 1992.